Mitochondrial-targeting nitrooxy-doxorubicin: a new approach to overcome drug resistance.

Chiara Riganti [1,2,*], Barbara Rolando [3], Joanna Kopecka [1,2], Ivana Campia [1,2], Konstantin Chegaev [3], Loretta Lazzarato [3], Antonella Federico [3], Roberta Fruttero [3], Dario Ghigo[1,2]

[1] Department of Oncology, University of Torino, via Santena 5/bis, 10126, Torino, Italy

[2]Center for Experimental Research and Medical Studies (CeRMS), University of Torino, via Santena 5/bis, 10126, Torino, Italy

[3] Department of Science and Drug Technology, University of Torino, via Pietro Giuria 9, 10125, Torino, Italy

*** Corresponding author:** Dr. Chiara Riganti, Department of Oncology, University of Torino; Via Santena 5/bis, 10126 Torino, Italy; phone: +39-011-6705857; fax: +39-011-6705845; email: chiara.riganti@unito.it

Abstract

In previous studies we showed that nitric oxide (NO) donors and synthetic doxorubicins (DOXs) modified with moieties containing NO-releasing groups - such as nitrooxy-DOX (NitDOX) or 3-phenylsulfonylfuroxan-DOX (FurDOX) - overcome drug resistance by decreasing the activity of ATP-binding cassette (ABC) transporters that can extrude the drug. Here we have investigated the biochemical mechanisms by which NitDOX and FurDOX exert antitumor effects.

Both NitDOX and FurDOX were more cytotoxic than DOX against drug-resistant cells. Interestingly, NitDOX exhibited a faster uptake and an extranuclear distribution. NitDOX was preferentially localized in the mitochondria, where it nitrated and inhibited the mitochondria-associated ABC transporters, decreased the flux through the tricarboxylic acid cycle, slowed down the activity of complex I, lowered the synthesis of ATP, induced oxidative and nitrosative stress, elicited the release of cytochrome c and the activation of caspase-9 and -3 in DOX-resistant cells. We suggest that NitDOX may represent the prototype of a new class of multifunctional anthracyclines, which have cellular targets different from conventional anthracyclines and greater efficacy against drug-resistant tumors.

Keywords: multifunctional drugs; doxorubicin; nitric oxide; multidrug resistance; ATP-binding cassette transporters; mitochondria

Introduction

Doxorubicin (DOX), also known as adriamycin, is an antibiotic belonging to the class of anthracyclines, widely used to treat solid and hematological malignancies. The molecular mechanisms that underlie the DOX anticancer effects include DNA damage, inhibition of topoisomerase II, induction of oxidative stress (synthesis of reactive oxygen species, ROS, and reactive nitrogen species, RNS), altered metabolism of Ca^{++} ions, and activation of host immune system against the tumor [1].

The limitations to DOX efficacy in cancer therapy are of two types: cardiotoxicity, which can occur as both acute and chronic dose-related forms, and development of resistance through different mechanisms, the main of which is the overexpression of ATP-binding cassette (ABC) transporters, such as P-glycoprotein (Pgp/ABCB1), multidrug resistance-associated proteins (MRPs/ABCCs) and breast cancer resistance protein (BCRP/ABCG2), which actively extrude the drug from tumor cells [2]. Resistance to DOX is often part of a cross-resistance towards several anti-cancer drugs known as multidrug resistance (MDR), that affects up to 70% tumors at diagnosis and increases in relapses and metastasis [3]. MDR also affects new molecularly-targeted drugs [4] and until now no satisfactory reversing strategies have been identified.

Previous works from our group showed that nitric oxide (NO) donors, such as sodium nitroprusside (SNP), *S*-nitrosopenicillamine, *S*-nitrosoglutathione [5,6], and furoxan derivatives (1,2,5-oxadiazole 2-oxides) [7], reverse MDR in human cancer cells. These compounds decreased the activity of Pgp/ABCB1 and MRPs/ABCCs pumps by nitrating critical tyrosines, thus allowing the increase of intracellular DOX accumulation and toxicity [5,6].

NO is a small molecule involved in the regulation of vascular tone, aggregation of platelets, angiogenesis, cell death, differentiation, neurotransmission, and activity of immune system [8]. It is synthesized from L-arginine by three NO synthase (NOS; EC 1.14.13.39) enzymes [9]. The role of NO in tumors, where it can be produced by cancer cells or by infiltrating macrophages [10], is matter of huge debate [11]. At nanomolar concentrations, NO is a tumor-growth supporter [12,13]. At

micromolar concentrations, as occurs after the up-regulation of inducible NOS (iNOS/NOS II), NO is an anti-tumor agent, which elicits oxidative damage on DNA, inactivates DNA-repairing systems, induces apoptosis and endoplasmic reticulum stress, hampers the mitochondrial energy metabolism, exerts anti-angiogenic effects, and enhances the reaction of host immune system against the tumor [14]. Beside its MDR-reversing properties, NO can enhance the efficacy of radiotherapy [15] and chemotherapy [16,17].

We have previously produced synthetic DOXs containing NO-releasing groups, such as nitrooxy-Doxorubicin (NitDOX, Supplementary Figure S1) and 3-phenylsulfonylfuroxan-Doxorubicin (FurDOX, Supplementary Figure S1), able to nitrate the MRP3/ABCC3 pump and to reduce the efflux of DOX in drug-resistant cells at low micromolar concentrations [18]. The NO-releasing groups selected differ in terms of kinetics and extent of NO released. The furoxan system can release NO under the action of endogenous thiols with mechanism not yet fully understood; by contrast, NO release from organic nitrates occurs through enzymatic catalysis. A number of enzymes have been proposed for this conversion: in particular, the role of mitochondrial aldehyde dehydrogenase and P-450 enzyme(s) has been emphasized [18].

The use of multi-target drugs or multifunctional drugs, namely single compounds capable of interacting simultaneously with more than one target, has lower risk of drug-drug interactions, improves compliance by the patient, and shows a more predictable pharmacokinetic profile compared with the association of drugs [19]. The development of resistance towards multi-target drugs is also expected to be more difficult. In addition, the NO-releasing multifunctional drugs should take advantage from the anti-cancer effects that both NO and DOX have and maximize the anti-tumor efficacy.

The aim of this work was to investigate how the presence of either the nitrooxy- or the 3-phenylsulfonylfuroxan group may improve and/or change the anticancer activity of DOX. We found that NitDOX is a lead compound with an unexpected and novel mechanism of action, which makes it an anthracycline exhibiting pharmacologic properties widely different from DOX.

Experimental Section

Chemicals.

Fetal bovine serum (FBS) and culture medium were supplied by Invitrogen Life Technologies (Carlsbad, CA); plasticware for cell cultures was from Falcon (Becton Dickinson, Franklin Lakes, NJ). Electrophoresis reagents were obtained from Bio-Rad Laboratories (Hercules, CA); the protein content of cell monolayers and lysates was assessed with the BCA kit from Sigma Chemical Co (St.Louis, MO). Those are not specified were purchased from Sigma Chemical Co. The synthesis of NitDOX and FurDOX were performed as described previously [18]. The structures are reported in Supplementary Figure S1, along with the methyl ester of acid containing nitrooxy moiety (NitE) and the methyl ester of acid containing phenylsulfonylfuroxan moiety (FurE).

Cell lines

Human colon cancer DOX-sensitive HT29 cells were cultured in RPMI 1640 medium. A subpopulation of DOX-resistant HT29 cells, named HT29-dx, was created as previously reported [5] and subsequently cultured in RPMI 1640 medium containing 200 nmol/L DOX. Human DOX-sensitive lung cancer A549 cells and human DOX-resistant lung cancer A549-dx cells (selected from the parental A549 cells after 30 passages in the presence of 50 nmol/L DOX) were grown in Ham's F12 medium. Human DOX-sensitive chronic leukemia K562 cells and human DOX-resistant K562-dx cells (selected from the parental cells after 30 passages in the presence of 25 pmol/L DOX) were grown in RPMI 1640 medium. Non transformed mesothelial Met5A cells were cultured in RPMI 1640; primary malignant mesothelioma MM98 cells, which have a constitutively resistant phenotype [20], were maintained in Ham's F12 medium. Rat cardiomyocytes H9c2 cells were grown in DMEM medium. Human epithelial colon CCD-18Co cells were cultured in MEM medium. All the culture media were supplemented with 10% FBS, 1% penicillin-streptomycin and 1% L-glutamine. Cell cultures were maintained in a humidified atmosphere at 37 °C and 5% CO_2.

Western blot analysis.

Cells were treated with boiling 0.5 mL lysis buffer (10 mmol/L Tris, 100 mmol/L NaCl, 20 mmol/L KH_2PO_4, 30 mmol/L EDTA, 1 mmol/L EGTA, 250 mmol/L sucrose, pH 7.5). After sonication 1 mmol/L $NaVO_4$, 1 mmol/L NaF, 10 mmol/L dithiothreitol (DTT) and the inhibitor cocktail set III (100 mmol/L AEBSF, 80 mmol/L aprotinin, 5 mmol/L bestatin, 1.5 mmol/L E-64, 2 mmol/L leupeptin and 1 mmol/L pepstatin; Calbiochem, La Jolla, CA) were added and cell lysates were centrifuged at 13,000×g for 15 min. 30 μg whole cell proteins were separated by SDS-PAGE and probed with the following antibodies: anti-Pgp/ABCB1 (Santa Cruz Biotechnology, Santa Cruz, CA), anti-MRP1/ABCC1 (Abcam, Cambridge, MA), anti-MRP2/ABCC2 (Abcam), anti-BCRP/ABCG2 (Santa Cruz Biotechnology), anti-SLC22A4 (Abcam), anti-actin (Sigma Chemical Co.). After an overnight incubation, the membrane was washed with PBS-Tween 0.1% v/v and subjected for 1 h to a peroxidase-conjugated secondary antibody (diluted 1:3000 in PBS-Tween with milk 5% w/v). The membrane was washed again with PBS-Tween, and proteins were detected by enhanced chemiluminescence (Immun-Star, Bio-Rad).

10 μg proteins from nuclear extracts or mitochondrial extracts (see below) were probed with the same antibodies, using respectively an anti-TATA Box Binding Protein (Santa Cruz Biotechnology) or an anti-VDAC/porin (Abcam) antibody, to check the equal control loading.

To analyze the presence of nitrated proteins, the whole cell extract was subjected to immunoprecipitation using a rabbit polyclonal anti-nitrotyrosine antibody (Millipore, Bedford, MA). Immunoprecipitated proteins were separated by SDS-PAGE and probed with anti-Pgp/ABCB1, anti-MRP1/ABCC1, anti-MRP2/ABCC2 or anti-BCRP/ABCG2 antibodies, as previously described.

Extracellular lactate dehydrogenase (LDH) activity

To verify the cytotoxic effect of DOX, the extracellular medium was centrifuged at 12,000 × g for 15 min to pellet cellular debris, whereas cells were washed with fresh medium, detached with trypsin/EDTA, re-suspended in 0.2 ml of 82.3 mmol/L triethanolamine phosphate-HCl (pH 7.6) and sonicated on ice with two 10 s bursts. LDH activity was measured in the extracellular medium and in the cell lysate, as reported [20]. The reaction was followed for 6 min, measuring absorbance at 340 nm with Packard EL340 microplate reader (Bio-Tek Instruments, Winooski, VT) and was linear throughout the time of measurement. Both intracellular and extracellular enzyme activity was expressed in μmol NADH oxidized/min/dish, then extracellular LDH activity was calculated as percentage of the total LDH activity in the dish.

Nitrite production

Confluent monolayers in 35 mm-diameter Petri dishes were incubated in fresh medium under the experimental conditions indicated in Results. Nitrite production was measured by adding 0.15 mL of cell culture medium to 0.15 mL of Griess reagent in a 96-well plate, and after a 10 min incubation at 37°C in the dark, the absorbance was detected at 540 nm with a Packard EL340 microplate reader (Bio-Tek Instruments). A blank was prepared for each experiment in the absence of cells, and its absorbance was subtracted from the one obtained in the presence of cells. Nitrite concentration was expressed as nmol/mg cell proteins.

Intracellular doxorubicin accumulation

The amount of DOX of whole cells lysates, nuclear and mitochondrial extracts was measured fluorimetrically as described [5], using a PerkinElmer LS-5 spectrofluorimeter (PerkinElmer, Waltham, MA). Excitation and emission wavelengths were 475 and 553 nm, respectively. A blank was prepared in the absence of cells in each set of experiments and its fluorescence was subtracted from the one measured in each sample. Fluorescence was converted in nmol DOX/mg cell proteins using a calibration curve prepared previously.

Topoisomerase II assay.

The *in vitro* activity of topoisomerase II was measured using the Topoisomerase II Drug Screening Kit (Topogen Inc, Port Orange, FL), following the manufacturer's instructions. 250 ng of the supercoiled pHOT1 plasmid were incubated with 5 U of purified human Topoisomerase IIa (TOPOGen Inc) at 37°C for 30 min, in the presence of DOX, NitDOX or etoposide. The reaction was stopped with SDS 10% w/v and 1 μg proteinase K was added in each tube. The products were resolved on a 1% w/v agarose gels, stained with 0.01% v/v ethidium bromide. The appearance of a band corresponding to linearized plasmid was taken as an index of active topoisomerase II. As control of the enzyme specificity, supercoiled pHOT1 was incubated in the absence of topoisomerase II and treated as reported above.

Doxorubicin uptake.

Drug uptake was measured as described in [21], with minor modifications. Cells were washed and pre-incubated for 5 min at 37°C in uptake buffer (125 mmol/L NaCl, 20 mmol/L $NaHCO_3$, 3 mmol/L KCl, 1.8 mmol/L $CaCl_2$, 1 mmol/L KH_2PO_4, 1.2 mmol/L $MgSO_4$, 10 mmol/L glucose, 10 mmol/L Hepes, pH 7.4), then incubated for 10 min with DOX or NitDOX, in the absence or presence of tetraethylammonium (TEA) chloride. The assay was stopped by diluting 1:10 the sample in ice-cold uptake buffer. Cells were detached and centrifuged at 13,000 x g for 30 s, washed three times with 1 mL ice-cold uptake buffer, lysed in 1 mL ethanol/0.3 N HCl and sonicated. The DOX amount was measured fluorimetrically as reported above.

Octanol/water partition coefficient determination.

The lipophilicity of DOX and NitDOX was estimated by measuring their partitioning between *n*-octanol and water buffered at pH 7.4. The distribution coefficients (log $D^{7.4}$s) were obtained by shake-flask technique at room temperature. The organic (*n*-octanol) and aqueous phase (50 mmol/L

phosphate buffer, pH=7.4; ionic strength adjusted to 0.15 mol/L with KCl) were mutually saturated by shaking for 4 h. The compounds were solubilised in the buffered aqueous phase at a concentration of about 0.1 mmol/L and an appropriate amount of *n*-octanol was added. The two phases were shaken for about 30 min, by which time the partitioning equilibrium of solutes is reached, and then centrifuged (10,000 x g 10 min). The concentration of the solutes was measured in the aqueous phase by reverse phase-HPLC. Each log D value is an average of at least six measurement. All the experiments were performed avoiding exposure to light.

Confocal microscope analysis.

5×10^5 cells were grown on sterile glass coverslips and treated as described in the Results section, then rinsed with PBS, fixed with 4% w/v paraformaldehyde for 15 min, washed three times with PBS and incubated with 4′,6-diamidino-2-phenylindole dihydrochloride (DAPI, diluted 1: 20,000) for 3 min at room temperature in the dark. Fluorescently labelled cells were washed three times with PBS and once with water, then the slides were mounted with 4 µl of Gel Mount Aqueous Mounting and examined. In the experiments concerning NitDOX intracellular localization, cells were previously transfected with expression vectors encoding for the GFP-fused-leader sequence of E1α pyruvate dehydrogenase to label mitochondria, the GFP-fused-KDEL sequence of calreticulin to label endoplasmic reticulum, the GFP-fused N-acetylgalactosaminyltransferase 2 to label Golgi apparatus (Cell Light BacMan 2.0, Invitrogen), then incubated for 6 h with 10 µM NitDOX and prepared for the analysis by confocal microscope as reported above. For each experimental point, a minimum of 5 microscopic fields were examined.

Cytosol-nucleus separation.

The cytosolic and nuclear extracts were prepared as reported previously[20]. After protein quantification, samples were stored at -80°C until use.

Mitochondria isolation and complex I-IV activity.

Mitochondria were extracted as described earlier [22]. A 50 μL aliquot was sonicated and used for the measurement of protein content or Western blotting; the remaining part was stored at -80°C until use. To confirm the presence of mitochondrial proteins in the extracts, 10 μg of each sonicated sample were subjected to SDS-PAGE and probed with an anti-VDAC/porin antibody (data not shown).

The activity of the mitochondrial complexes I-IV was measured on 10 μg of non-sonicated mitochondrial extracts, as reported [23]. Each reaction was followed for 5 min, using a Lambda 3 spectrophotometer (PerkinElmer).

HPLC and LC-ESI-MS analyses of cell fractions.

DOX or NitDOX were incubated for 24 h in HT29 cells at 10 μmol/L to operate at a concentration that granted the optimal sensitivity of HPLC analysis. The reverse-phase (RP) HPLC procedure allowed the separation and quantitation of compounds and degradation products in cytosolic, nuclear, and mitochondrial fractions. Cellular fractions were obtained as described above and diluted with equal volume of acetonitrile in order to deproteinize the sample. The sample was sonicated, vortexed and then centrifuged for 10 min at 2,150 x g, the clear supernatant was filtered by 0.45 μm polytetrafluoroethylene filters and analysed by RP-HPLC or LC-ESI-MS methods. HPLC analyses were performed with a HP 1100 chromatograph system (Agilent Technologies, Palo Alto, CA, USA) equipped with a quaternary pump (model G1311A), a membrane degasser (G1379A), a diode-array detector (DAD) (model G1315B) integrated in the HP1100 system. Data analyses were processed using a HP ChemStation system (Agilent Technologies). The analytical column was a HyPurity Elite C18 (250×4.6mm, 5 μm; Hypersil, ThermoQuest Corporation, UK). The mobile phase consisting of acetonitrile/phosphate buffer (50 mmol/L, pH 2.0) at flow-rate = 1.0 mL/min with gradient conditions: 70% PBS until 5 min, from 70 to 35% PBS between 5 and 15 min, and from 35 to 70% PBS between 15 and 20 min. The injection volume was 100 μL

(Rheodyne, Cotati, CA). The column effluent was monitored at 234 mn and 480 nm referenced against a 700 nm wavelength. Quantitation of DOX and NitDOX was done using calibration curves of compounds: the linearity of the calibration curves was determined in a concentration range of 1-50μM ($r^2 > 0.99$); quantitative analysis of their metabolites was also conducted using DOX (for doxorubicinol) and NitDOX (for denitrated derivatives) as references.

LC-ESI-MS analyses were performed with a Thermo Finningan LCQ Deca XP *plus* system equipped with a quaternary pump, a Surveyor AS autosampler, a Surveyor photodiode array detector and a vacuum degasser was used for LC/MS analyses (Thermo Electron Corporation, Waltham, MA). All the chromatographic separations were performed on a Hypersil HyPURITY™ Elite C18 (5 μm, 250 x 4.6 mm) (ThermoQuest Corporation, UK) as a stationary phase protected by a C18 SecurityGuard (Phenomenex srl, Castel Bolognese, Italy). Aliquots (20 μL) of supernatants obtained from incubations were injected onto the system and eluted with a mobile phase (flow rate 0.8 mL/min) consisting of a A: 0.1% formic acid solution, B: acetonitrile. The following gradient elution was used: 0 to 5 min [A= 65%, B=35%], 5 to 17 min [A= 30%, B=70%], 17 to 17.5 min [A= 65%, B=35%], and 17.5 to 25 min [A= 65%, B=35%]. The eluants were filtered through a 0.45-μm pore size polyvinylidene difluoride membrane filter before use. The eluate was injected into the electrospray ion source (ESI) and MS spectra were acquired and processed using Xcalibur® software. The operating conditions on the ion trap mass spectrometer were as follows: *Positive mode:* spray voltage, 5.30 kV; source current, 80 μA; capillary temperature, 350 °C; capillary voltage, 12.00 V; tube lens offset, -30.00 V; multipole 1 offset, -6.75 V; multipole 2 offset, -8.50 V; sheath gas flow (N_2), 60 Auxiliary Units. Data was acquired in full-scan and product ion scan modes (MS^2) using mass scan range *m/z* 200-900. The collision energy was optimized at 25%.

Tricarboxylic acid (TCA) cycle measurement.

Cells were washed with PBS, detached with trypsin/EDTA and resuspended at 2 x 10^5 cells in 1 mL of Hepes buffer (145 mmol/L NaCl, 5 mmol/L KCl, 1 mmol/L MgSO4, 10 mmol/L Hepes, 10

mmol/L glucose, 1 mmol/L $CaCl_2$, pH 7.4) containing 2 μCi of [6-^{14}C]glucose (55 mCi/mmol, PerkinElmer). Cell suspensions were incubated for 1 h in a closed experimental system to trap the $^{14}CO_2$ developed from [^{14}C]glucose and the reaction was stopped by injecting 0.5 mL 0.8 N $HClO_4$. The amount of glucose transformed into CO_2 through the TCA cycle was calculated as described [24] and expressed as nmol CO_2/h/mg of cell proteins.

ATP synthesis.

Quantitative determination of ATP in mitochondria was performed using the ATP Bioluminescent Assay Kit (FL-AA, Sigma Aldrich Co.), following the manufacturer's instruction. The luminescence was recorded using a Magic Lite Analyzer (Ciba Corning Diagnostic Corp., Cambridge, MA). ATP was quantified as arbitrary light units and then converted into nmol ATP/mg mitochondrial proteins, according to a calibration curve previously set.

ROS and RNS measurement.

For ROS measurement, cells were rinsed with PBS and loaded with 10 μmol/L 5-(and-6)-chloromethyl-2',7'-dichorodihydro-fluorescein diacetate-acetoxymethyl ester (DCFDA-AM) for 10 min at 37°C, then washed and re-suspended in 0.5 mL PBS. The intracellular fluorescence was detected by flow cytometry, using a FACSCalibur system (Becton Dickinson), with a 530 nm bandpass filter. For each analysis 100,000 events were collected and analyzed by the CellQuest software (Becton Dickinson).

The amount of intracellular nitrotyrosine, considered as an index of RNS generation [25], was measured by the Nitrotyrosine ELISA kit (Hycult Biotechnolohgy, The Netherlands), following the manufacturer's instructions. The absorbance was read with a Packard EL340 microplate reader (Bio-Tek Instruments) and converted into pmol/mg cell proteins according to the titration curve.

Lipid peroxidation.

Cells were washed with fresh medium, detached and re-suspended in 1 mL of PBS. Lipid peroxidation was detected by measuring the intracellular level of malonyldialdehyde (MDA), an end product of polyunsaturated fatty acids and related esters breakdown, with the Lipid Peroxidation Assay kit (Oxford Biomedical Research, Oxford, MI), which uses the reaction of *N*-methyl-2-phenylindole with MDA in the presence of hydrochloric acid to yield a stable chromophore with maximal absorbance at 586 nm. The absorbance was measured with a Packard EL340 microplate reader (Bio-Tek Instruments). Results were expressed as nmol/mg cell proteins, according to a titration curve previously prepared.

Cytochrome c release.

10 μg of proteins from cytosolic and mitochondrial fraction were subjected to Western blotting to assess the cytosolic release of cytochrome c, taken as an index of apoptosis [26], using an anti-cytochrome c antibody (Becton Dickinson).

Caspase activity.

Cells were lysed in 0.5 mL of caspase lysis buffer (20 mmol/L Hepes/KOH, 10 mmol/L KCl, 1.5 mmol/L $MgCl_2$, 1 mmol/L EGTA, 1 mmol/L EDTA 1, 1 mmol/L DTT, 1 mmol/L PMSF, 10 μg/mL leupeptin, pH 7.5). 20 μg cell lysates were incubated for 1 h at 37°C with 20 μmol/L of the fluorogenic substrate of caspase-9 Ac-Leu-Glu-His-Asp-7-amino-4-methylcoumarin (LEHD-AMC) or of caspase-3 Ac-Asp-Glu-Val-Asp-7-amino-4-methylcoumarin (DEVD-AMC), in 0.25 mL caspase assay buffer (25 mmol/L Hepes, 0.1 % w/v 3-[(3-cholamidopropyl)dimethylammonio]-1-propanesulfonate (CHAPS), 10% w/v sucrose, 10 mmol/L DTT, 0.01% w/v egg albumin, pH 7.5). The reaction was stopped by adding 0.75 mL ice-cold 0.1% w/v trichloroacetic acid and the fluorescence of AMC fragment released by active caspases was read using a LS-5 spectrofluorimeter (PerkinElmer). Excitation and emission wavelengths were 380 nm and 460 nm,

respectively. Fluorescence was converted in pmol/μg cell proteins, using a calibration curve prepared previously with standard solutions of AMC.

Statistical Analysis.

All data in text and figures are provided as means ± SD. The results were analyzed by a one-way analysis of variance (ANOVA) and Tukey's test. $p < 0.05$ was considered significant.

Results

Nitrooxy-doxorubicin is more effective than doxorubicin in drug-resistant cancer cells.

To monitor the intracellular drug accumulation and toxicity of DOX, NitDOX and FurDOX, we chose the model of the drug-sensitive human colon cancer HT29 cells and the drug-resistant counterpart HT29-dx cells, which express higher levels of several ABC transporters extruding DOX, such as Pgp/ABCB1, MRP1/ABCC1, MRP2/ABCC2 and BCRP/ABCG2, than HT29 cells (Figure 1A). At 5 μmol/L, a concentration of DOX that was cytotoxic in HT29 cells, but not in HT29-dx cells [5], all the drugs accumulated time-dependently in HT29 cells, with FurDOX > NitDOX > DOX (Figure 1B). DOX was not retained in HT29-dx cells, in contrast to NitDOX and FurDOX whose accumulation increased as function of time also in drug-resistant cells. The content of FurDOX was higher than that of NitDOX at each time point (Figure 1B). A similar trend was observed for the extracellular nitrite amount (Figure 1C), taken as an index of NO released by the compounds (for NitDOX and FurDOX) or synthesized by the cells themselves: DOX induced a significant increase of nitrite only in HT29 cells after 24 h, whereas with NitDOX and FurDOX the NO levels were higher than with DOX, raised earlier and in both sensitive and resistant cells. FurDOX was a stronger NO releaser than NitDOX (Figure 1C). Cell toxicity, measured as the release of LDH in the extracellular medium, was produced by DOX only in HT29 cells and not in

HT29-dx cells; on the opposite, the NO-releasing drugs were cytotoxic both in drug-sensitive and drug-resistant cells (Figure 1D).

Figure 1

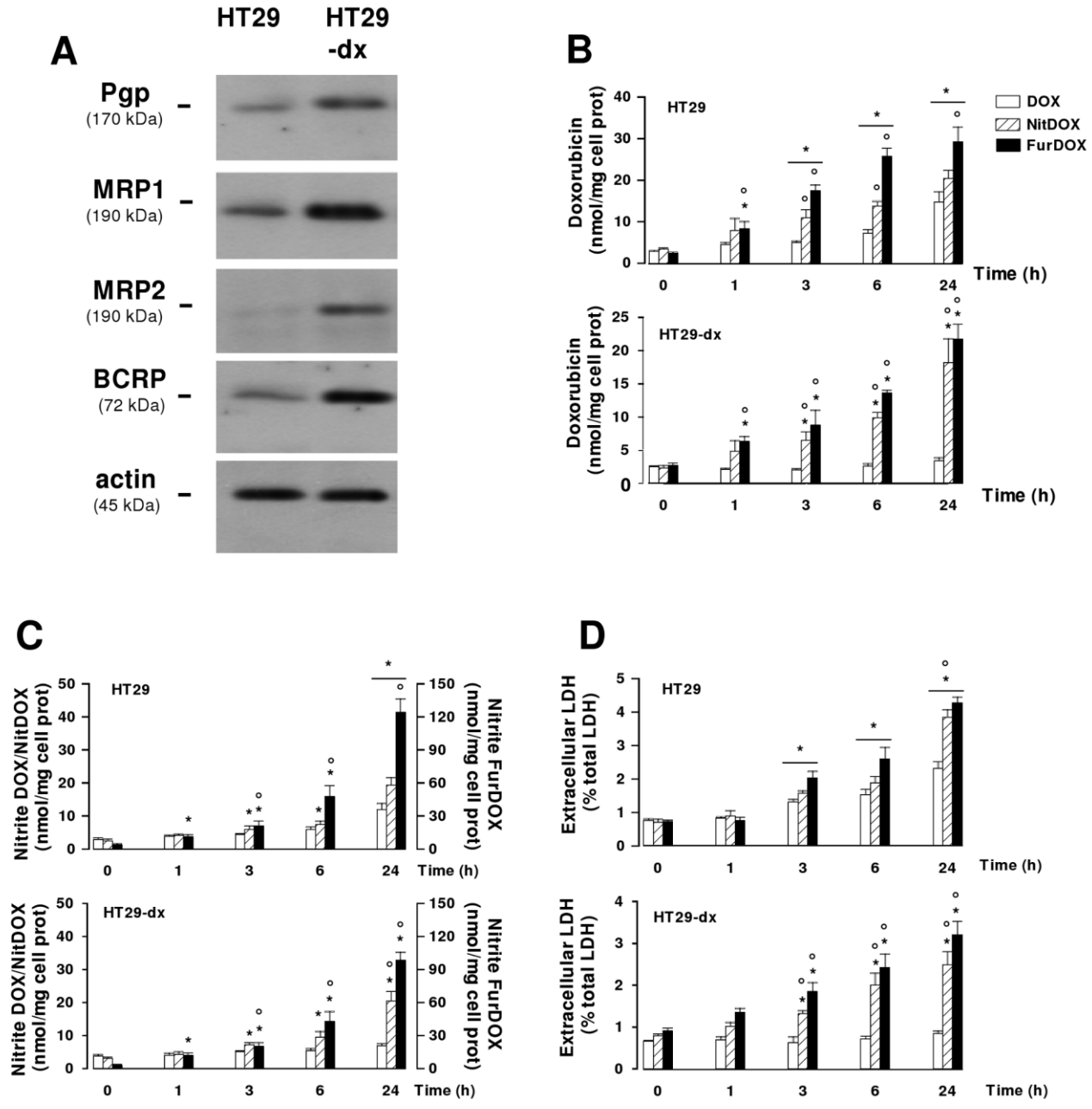

To clarify whether NO was the main responsible of the cytotoxicity of the compounds, in a parallel experimental set we used DOX in association with different NO-donors - i.e. the methyl ester of acid containing nitrooxy moiety (NitE), the methyl ester of acid containing phenylsulfonylfuroxan

moiety (FurE), SNP, spermine NONOate (NONO) -, each showing different kinetics and potency of NO release (Supplementary Figure S2A). All the NO-donors increased the intracellular retention of DOX at 24 h (Supplementary Figure S2B); the most potent NO-donors (FurE and NONO) were also the most potent enhancers of the intracellular accumulation of DOX (Supplementary Figure S2B). They were also cytotoxic *per se* in HT29 and HT29-dx cells (Supplementary Figure S2C). Of note, the presence of NO-donors restored the cytotoxicity of DOX in drug-resistant HT29-dx cells (Supplementary Figure S2C).

After 24 h cells treated with NitE or FurE had similar levels of nitrite when compared to cells treated with NitDOX or FurDOX (compare Supplementary Figure S2A and Figure 1C). Also the DOX content was superimposable between the experimental conditions DOX + NitE and NitDOX, or DOX + FurE and FurE (compare Supplementary Figure S2B and Figure 1B). Unexpectedly, the release of LDH was higher with NitDOX than with DOX + NitE, as well as with FurDOX than with DOX + FurE (compare Supplementary Figure S2C and Figure 1D), suggesting that NitDOX and FurDOX may have additional mechanisms of toxicity than DOX co-incubated with the corresponding NO-releasing molecule.

NitDOX and FurDOX were significantly more accumulated than DOX also in other human cancer cells possessing an acquired drug-resistant phenotype, such as A549-dx and K562-dx cells (which, as expected, retained less DOX than the sensitive counterparts A549 and K562), and in primary cells of malignant mesothelioma (MM98), which again contained a lower amount of DOX than the non-transformed mesothelial cells Met5A (Supplementary Figure S3A).

We checked in parallel the release of LDH from H9c2 cardiomyocytes: whereas DOX and NitDOX did not differ for the intracellular accumulation and the toxicity, FurDOX was significantly more accumulated and elicited a stronger cytotoxic effect (Supplementary Figure S3B).

Similarly, in non transformed human colon epithelial CCD-18Co cells, DOX and NitDOX did not differ in terms of intracellular drug accumulation (Supplementary Figure S4A), nitrite and cytotoxicity (Supplementary Figure S4B), whereas FurDOX was the most retained within CCD-

18Co cells, the most potent inducer of NO and the most potent inducer of cytotoxicity (Supplementary Figure S4A-B).

In consequence of the higher toxicity of FurDOX in cardiomyocytes (Supplementary Figure S3B) and non transformed epithelial cells (Supplementary Figure S4B), we withdrew FurDOX from the subsequent experiments and focused our investigation on NitDOX, which was more effective than DOX in accumulating into all cell lines we analyzed, without exerting a greater toxicity than DOX on cardiomyocytes and non transformed colon cells.

Nitrooxy-doxorubicin does not inhibit topoisomerase II and has a different uptake and intracellular distribution than doxorubicin.

Since one of the anticancer mechanisms of DOX is the inhibition of topoisomerase II, we first investigated whether the addition of the nitrooxy group enhanced this property in an *in vitro* assay (Figure 2). Purified topoisomerase II was inhibited dose-dependently by DOX, as well as by etoposide, the other inhibitor profiled. NitDOX poorly inhibited topoisomerase II (Figure 2). This result led us to hypothesize that the cell toxicity of NitDOX relies on different mechanisms, such as more favorable kinetics of uptake or cellular targets different from nuclear topoisomerase II.

Figure 2

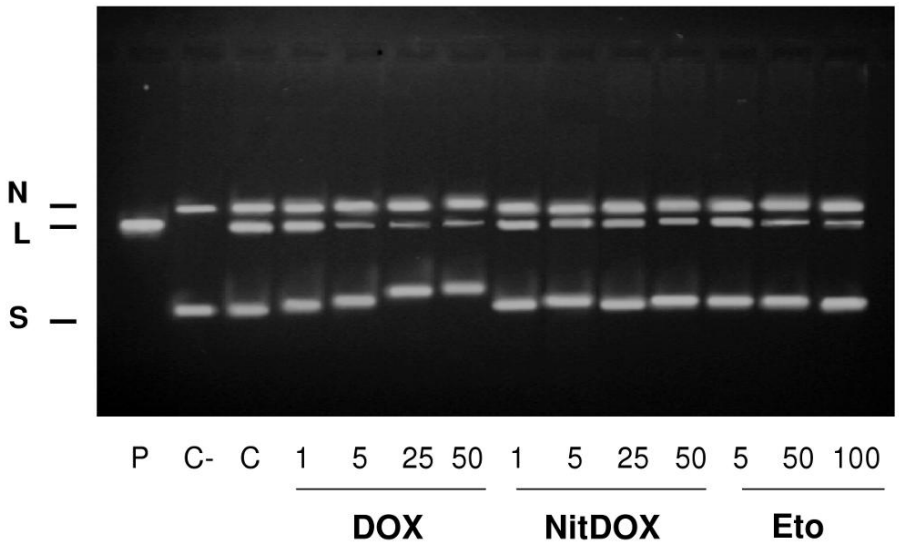

NitDOX was more rapidly uptaken than DOX (Figure 3A). The uptake of DOX was lower in HT29-dx cells (1.94 ± 0.19 nmol/mg prot, corresponding to 0.41 ± 0.06 µmol/L) than in HT29 cells (3.94 ± 0.43 nmol/mg prot, corresponding to 0.91 ± 0.03 µmol/L), whereas the entry of NitDOX was the same in drug-sensitive (4.74 ± 0.58 nmol/mg prot, corresponding to 1.14 ± 0.07 µmol/L) and drug-resistant cells (4.72 ± 0.91 nmol/mg prot, corresponding to 1.01 ± 0.09 µmol/L). In addition, the uptake of DOX was reduced in the presence of TEA (Figure 3A), an inhibitor of the SLC22A4 transporter, a member of the organic cation/zwitterion transporters family that mediates the entry of DOX by facilitated transport [21]. SLC22A4 was slightly higher in HT29 cells than in HT29-dx cells (Figure 3B). Since the uptake of NitDOX was equal in both cell lines and did not change in the presence of TEA (Figure 3A), it was likely a SLC22A4-independent process.

NO – endogenously produced or released from the nitrooxy group – was not responsible for the greater uptake of NitDOX, as suggested by the finding that the uptake of the compound was not reduced by NO scavengers, such as 2-phenyl-4,4,5,5-tetramethylimidazoline-1-oxyl 3-oxide (PTIO) or packed red blood cells. Similarly, NO scavengers did not affect the uptake of DOX (data not shown).

Another remarkable difference between DOX and NitDOX was the intracellular distribution: whereas DOX accumulated in the nuclei of HT29 cells, NitDOX exhibited a prominent extranuclear localization at 30 min, 1, 3, 6 h (data not shown) and 24 h (Figure 3C). The quantitative fluorimetric analysis of DOX and NitDOX in nuclear and cytosolic extracts confirmed what we had previously observed in whole HT29 cells (Figure 1D). In HT29-dx cells the amount of DOX was lower in both nuclei and cytosol (Figure 3D) and was undetectable by microscope analysis (data not shown). NitDOX, although a bit less accumulated in HT29-dx cells, maintained the same distribution pattern observed in HT29 cells, reaching the highest concentration in cytosolic fractions (Figure 3D). The co-incubation of DOX and NO-donors increased the amount of DOX in nuclear extracts, without significant differences between each compound (Supplementary Figure S5A). Only a small increase of DOX was detectable in cytosolic extracts (Supplementary Figure S5A).

Figure 3

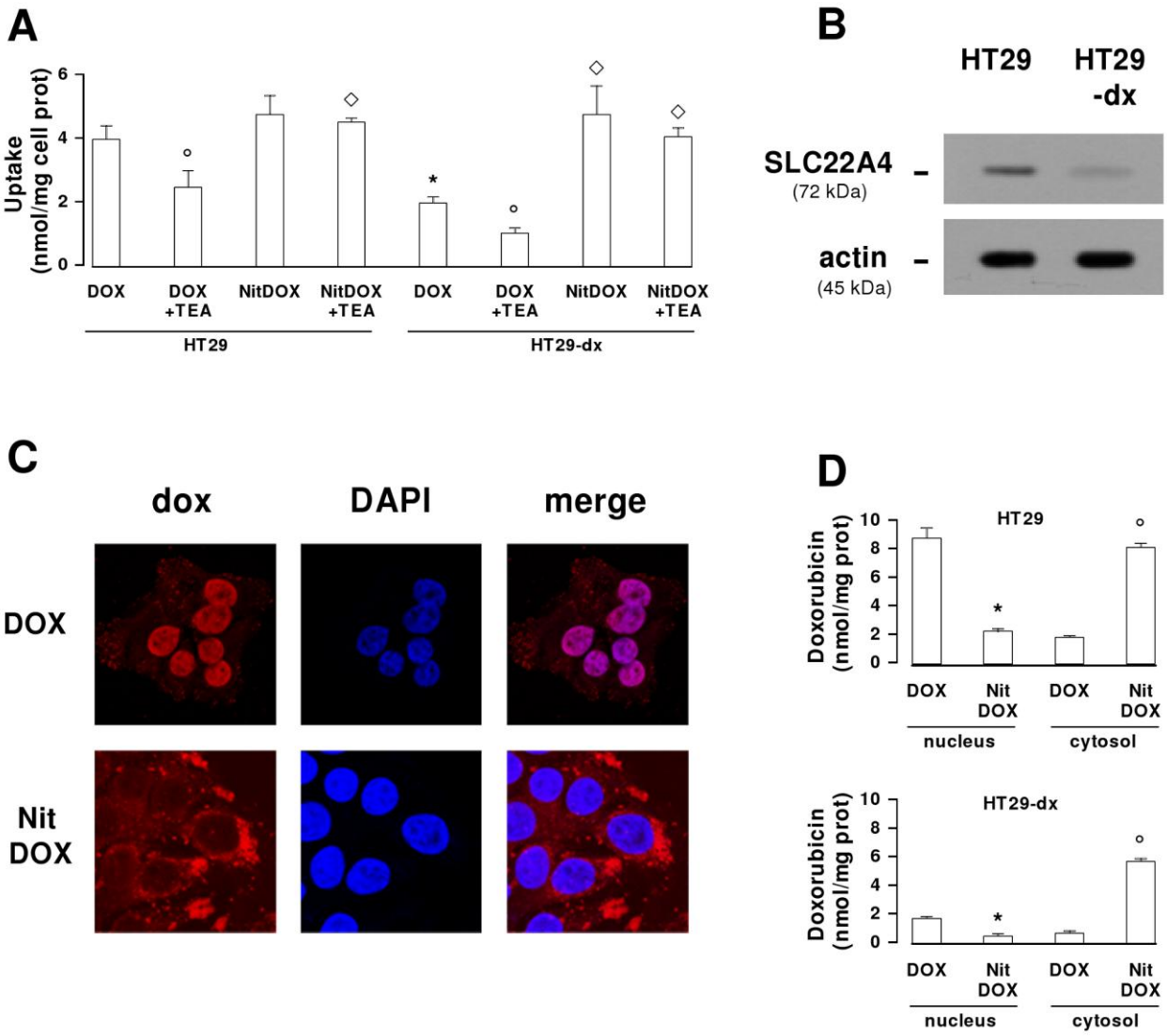

SLC224A was absent from nuclear extracts (data not shown) and TEA was devoid of effect on the drugs distribution (data not shown). Pgp/ABCB1, MRP1/ABCC1 and BCRP/ABCG2 were present in nuclear extracts and were nitrated by DOX in HT29 cells and by NitDOX in HT29 and HT29-dx cells (data not shown); however, PTIO, which prevented the nitration of the transporters, did not change the distribution of DOX or NitDOX (data not shown). These results indicate that the exclusion of NitDOX from nucleus was not due to a different uptake via SLC22A4 protein or to a different efflux from nuclear envelope mediated by ABC transporters.

DOX and NitDOX had a different lipohilicity: the octanol/water distribution coefficient at pH 7.4 (log $D^{7.4}$) was 0.47 $\pm$ 0.08 for DOX and 2.72 $\pm$ 0.09 for NitDOX (n =6), suggesting that NitDOX should be more favored to enter cells by a simple diffusion mechanism. The different hydrophobicity may explain also the different intracellular distribution of NitDOX and DOX. HPLC analysis of nuclear and cytosolic extracts from HT29 cells confirmed that DOX was mainly present in the nucleus and NitDOX outside it (Table 1; Supplementary Figure S6).

Nitrooxy-doxorubicin is localized to mitochondria and impairs mitochondria metabolism.

To gather more information about the intracellular localization of NitDOX, we transfected HT29 cells with GFP-fused-expression vectors targeting specific organelles: NitDOX was mainly found in mitochondria and endoplasmic reticulum, whereas it was absent from the Golgi apparatus (Figure 4A).

Interestingly, NitDOX reached the same concentration in mitochondria of HT29 and HT29-dx cells and was significantly higher than DOX (Figure 4B). Conversely, none of NO-donors increased the intramitochondrial accumulation of DOX, with the exception of a small but not significant increase promoted by NitE (Supplementary Figure S5B). Mitochondria of HT29 and HT29-dx cells have several ABC pumps transporting DOX, such as Pgp/ABCB1, MRP1/ABCC1, MRP2/ABCC2 and BCRP/ABCG2 (Figure 4C). Interestingly, the amount of MRP1/ABCC1 was higher in HT29-dx cells (Figure 4C): this element may explain the lower accumulation of DOX in the mitochondrial fraction of this cell population (Figure 4B). DOX in HT29 and NitDOX in both HT29 and HT29-dx cells elicited the tyrosine nitration of MRP1/ABCC1 and BCRP/ABCG2, an event that was prevented by the addition of PTIO (Figure 4C). SLC22A4 was not detectable nor TEA affected the intra-mitochondrial accumulation of DOX and NitDOX (data not shown).

Figure 4

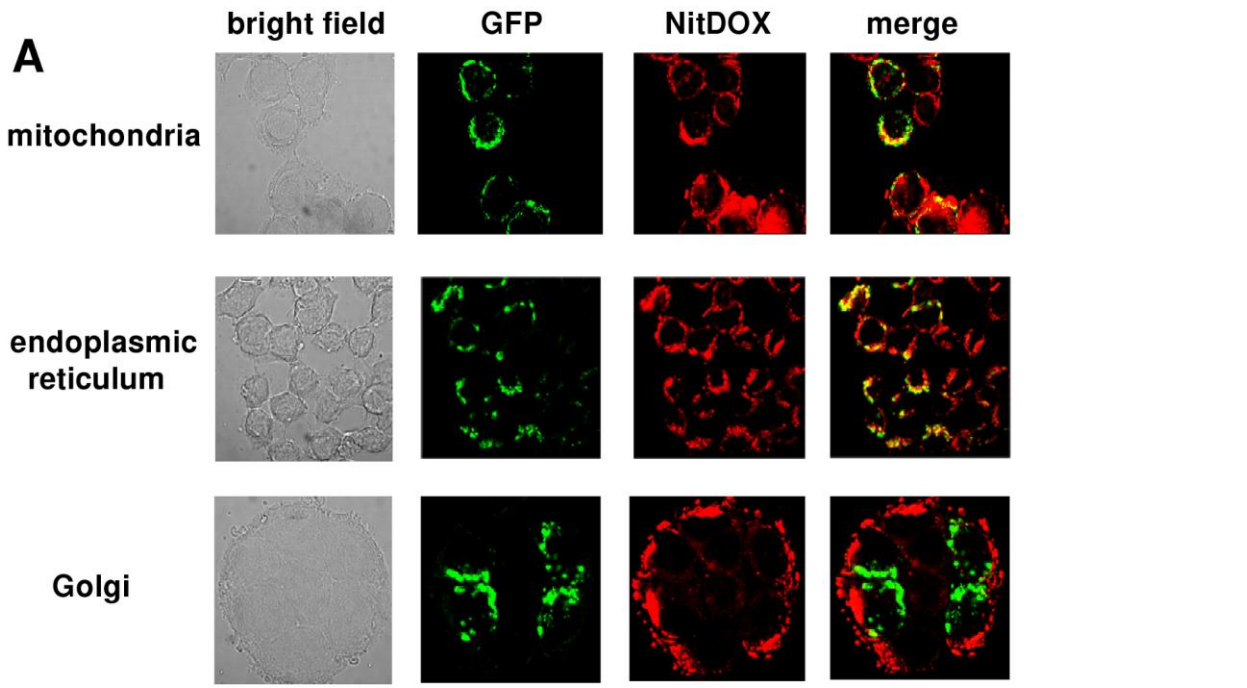

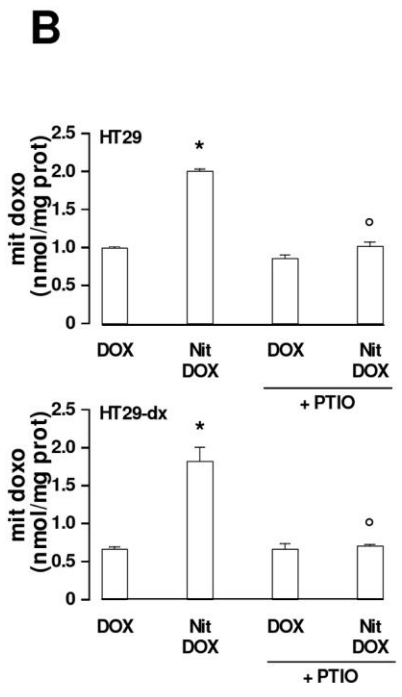

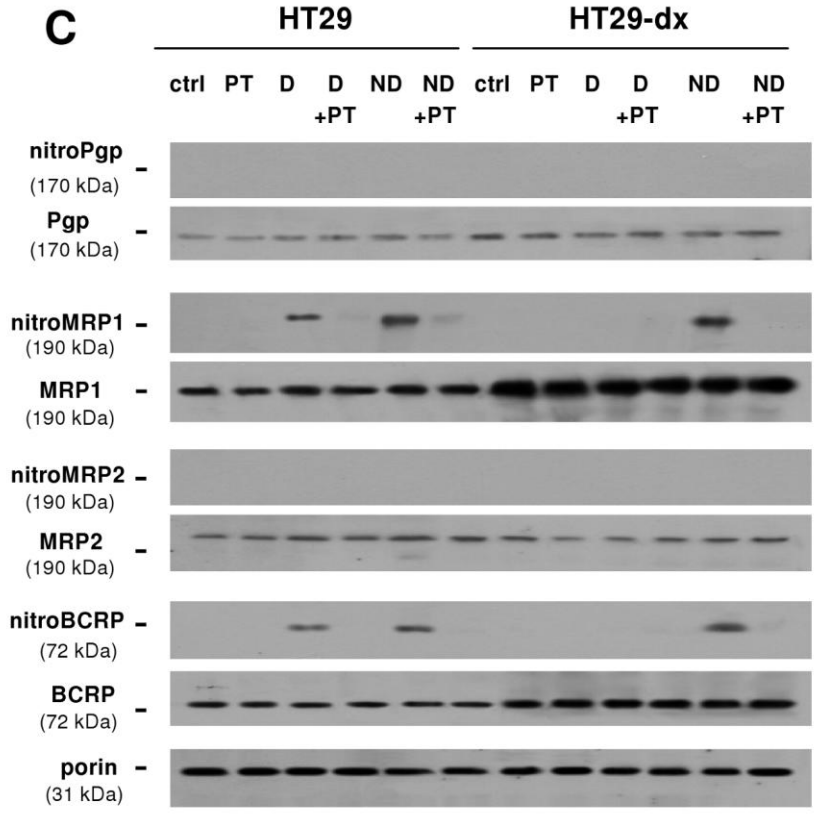

In HT29-dx cells the oxidative mitochondria metabolism was more active than in HT29 cells, as demonstrated by the higher flux through the TCA cycle (Figure 5A), the higher electron flux

through complex I (Figure 5B) and the higher synthesis of ATP (Figure 5F). In keeping with the different intramitochondrial accumulation, DOX reduced TCA flux, complex I activity and ATP synthesis in HT29 cells, but was devoid of effect in HT29-dx cells (Figure 5A, 5B and 5F), where it was poorly retained into mitochondria (Figure 4B). On the contrary, NitDOX, which accumulated in mitochondria of both drug-sensitive and drug-resistant cells (Figure 4B), equally decreased in these cells TCA cycle, complex I activity and ATP synthesis (Figure 5A, 5B and 5F). No changes occurred in the activity of other steps of mitochondrial electron chain, as determined by the electron flux through the segment complex I to III (Figure 5C), through the segment complex II to III (Figure 5D) and through complex IV (Figure 5E). These data suggest that the effects elicited by the anthracyclines on mitochondrial metabolism have rather specific targets. For both DOX in HT29 cells and NitDOX in HT29 and HT29-dx cells, the changes on TCA activity, complex I and ATP synthesis were abrogated by the addition of PTIO (Figure 5A, 5B and 5F).

Figure 5

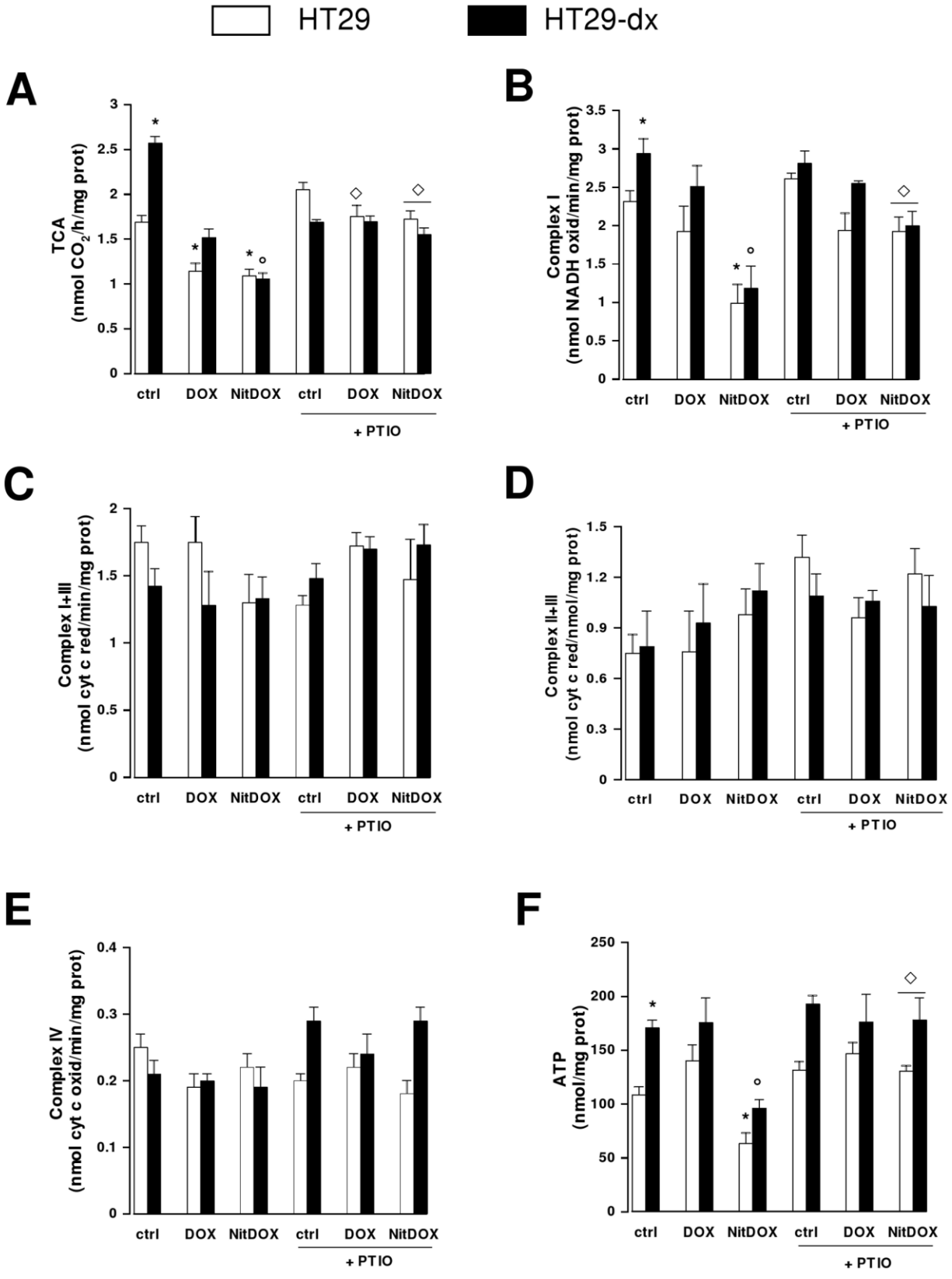
HT29
HT29-dx
A
TCA
(nmol CO_2/h/mg prot)
B
Complex I
(nmol NADH oxid/min/mg prot)
C
Complex I+III
(nmol cyt c red/min/mg prot)
D
Complex II+III
(nmol cyt c red/nmol/mg prot)
E
Complex IV
(nmol cyt c oxid/min/mg prot)
F
ATP
(nmol/mg prot)
ctrl
DOX
NitDOX
+ PTIO

Furthermore, the rate of DOX and NitDOX metabolism within mitochondria was different: in mitochondrial extracts of HT29 cells treated with DOX, we detected both DOX and a more hydrophilic metabolite, suggestive of doxorubicinol [27] (DOX-ol, Table 1; Supplementary Figures S6 and S7). On the contrary in mitochondria of NitDOX-treated cells, we found mainly NitDOX, together with DOX obtained from the hydrolysis of the ester group (about 14%), and a considerable percentage (about 25%) of the two denitrated metabolites deriving from NO release (NitDOX denitrate 1 and 2, Supplementary Figures S6 and S7). Structures of the metabolites generated from DOX and NitDOX are summarized in the Supplementary Figure S8.

Nitrooxy-doxorubicin exerts a strong oxidative/nitrosative stress and activates the intrinsic pathway of apoptosis in resistant cells.

DOX increased the amount of ROS (Figure 6A) and the amount of nitrotyrosine, indicator of RNS generation [25] (Figure 6B) in HT29 cells, but not in HT29-dx cells. These events however were not sufficient to produce significant oxidative damage, because no marked change in lipid peroxidation was detected (Figure 6C). On the contrary, NitDOX effectively raised the amount of ROS and RNS in HT29 well as well as in HT29-dx cells (Figure 6A and 6B). Accordingly, only NitDOX produced a strong oxidative damage in both cell lines, as suggested by the significant increase of MDA level (Figure 6C). NO was crucial in the genesis of this type of damage, since the effect of NitDOX was reduced by the addition of PTIO (Figure 6C).

Figure 6

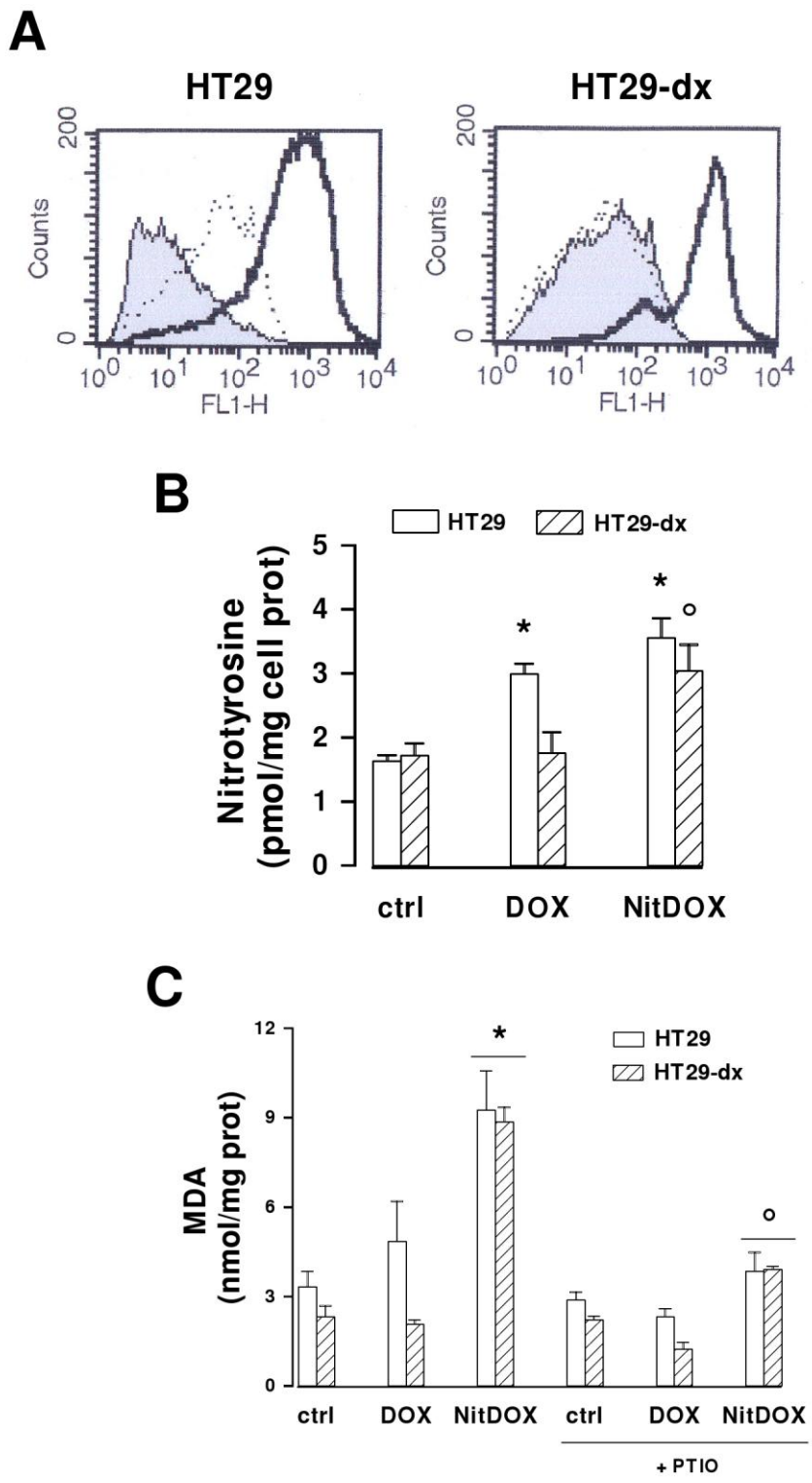

Finally, to determine whether the impairment of mitochondria metabolism and the increased oxidative damages elicited by NitDOX effectively resulted in cell death, we analyzed the release of

cytochrome c into the cytosol and the subsequent activation of the caspases involved in the intrinsic apoptotic pathway. Whereas DOX produced a small cytosolic release of cytochrome c (Figure 7A), followed by an increased activity of caspase-9 (Figure 7B) and caspase-3 (Figure 7C) only in HT29 cells, NitDOX was a stronger inducer of cytochrome c release (Figure 7A) and a stronger activator of caspase-9 (Figure 7B) and caspase-3 (Figure 7C) in both HT29 and HT29-dx cells. Again, the removal of NO by PTIO, prevented all the pro-apoptotic effects of DOX and NitDOX (Figure 7A-7C).

Figure 7

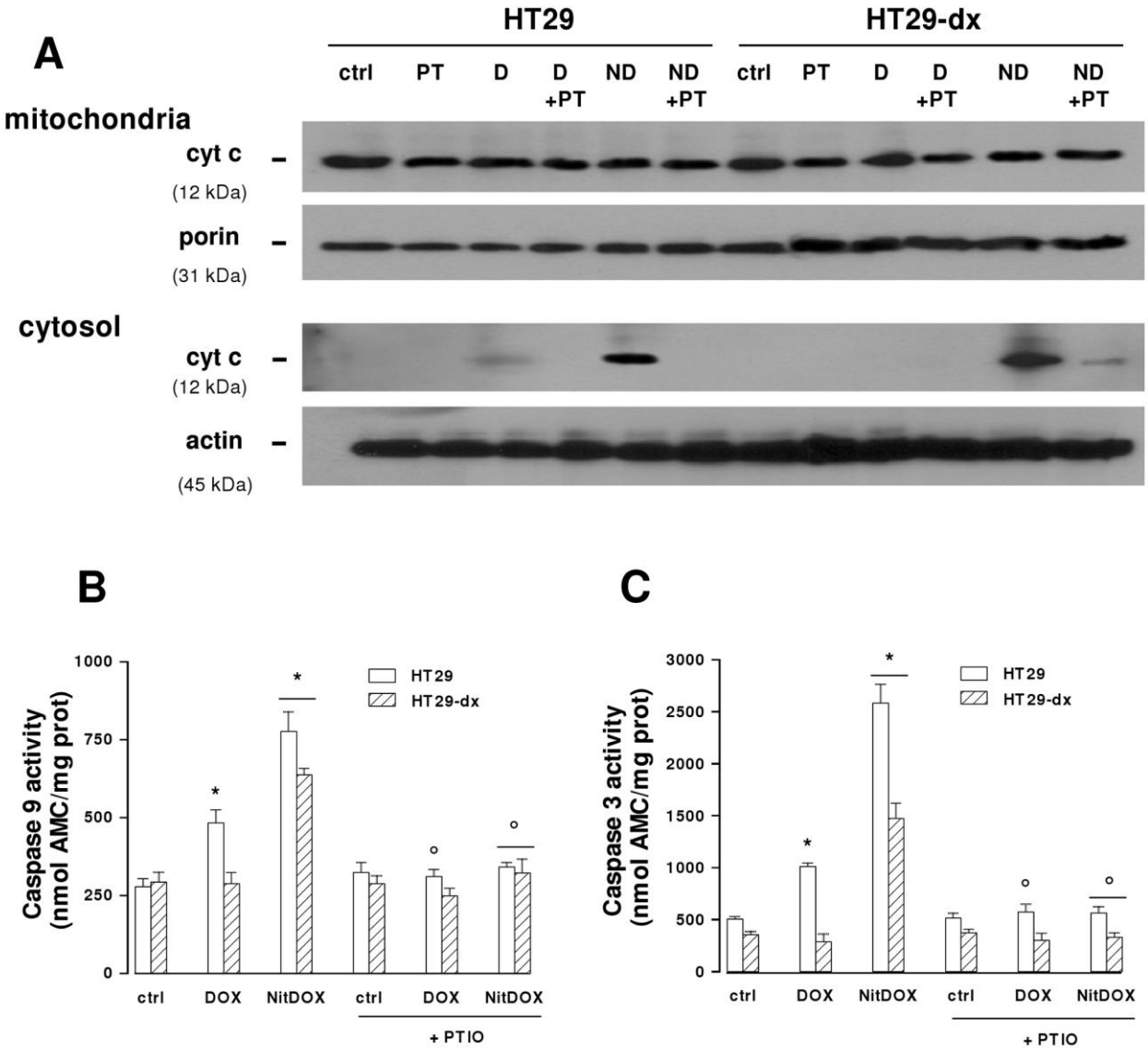

Discussion

In the light of previous studies showing that NO-donors are chemosensitizers [5,16,17], several NO-based strategies, such as the use of the ABC transporters inhibitors conjugated with NO [28] or the use of compounds with the dual property of inhibiting Pgp and increasing the endogenous synthesis of NO [29], have been investigated. We have recently synthesized new multifunctional DOXs by joining them - through an appropriate linker – to a NO-donor with known biological properties. These compounds, namely nitrooxy-DOX (NitDOX) and 3-phenylsulfonylfuroxan-DOX (FurDOX), overcame multidrug resistance in human colon cancer HT29-dx cells [18]. Given the pleiotropism of anti-cancer effects of NO [14], we hypothesized that NO-releasing DOXs may have additional effects than parental DOX.

Colon cancers are an interesting model to test this hypothesis, because they are particularly sensitive to the cytotoxic effects of NO. For instance, NO-conjugated non-steroidal anti-inflammatory drugs reduce tumor growth of colon cancer and induce apoptosis with a potency significantly higher than the parental non-steroidal anti-inflammatory drugs [30,31]. In our model of DOX-sensitive HT29 and DOX-resistant HT29-dx colon cancer cells incubated with DOX, NitDOX or FurDOX, the degree of toxicity was proportional to the amount of intracellular DOX and to the amount of NO released. Similarly, when we used DOX in association with different NO-donors, we increased in parallel the levels of nitrite, the intracellular accumulation of DOX and the cytotoxicity, restoring the DOX-induced cytotoxicity also in drug-resistant HT29-dx cells. Both the increased retention of DOX and the increased amount of NO, produced by inducible NO synthase in response to the intracellular DOX or released by the compounds, may explain this restoration of cytotoxicity in DOX-resistant cells. NitDOX and FurDOX, being less extruded than DOX by ABC transporters[18], achieved a good accumulation in both HT29 and HT29-dx cells. Their ability to release NO had the dual effect to further reduce the drug extrusion through the ABC transporters and to enhance the drug toxicity in resistant cells.

Interestingly the cytotoxicity elicited by NitDOX or FurDOX was higher than the cytotoxicity elicited by the same amount of DOX co-incubated with the corresponding NO-releasing molecule (i.e. the methyl ester of acid containing nitrooxy moiety NitE and the methyl ester of acid containing phenylsulfonylfuroxan moiety FurE, respectively). This result suggested that the cytotoxicity of NitDOX and FurDOX was not simply the sum of increased NO release and increased retention of DOX, but resulted from different pharmacodynamic effects.

FurDOX, the most effective NO-releasing DOX against drug-resistant cells, was also highly cytotoxic for cardiomyocytes *in vitro*, while conversely NitDOX was not more toxic than DOX. The protective or toxic effects of NO on cardiomyocytes are difficult to predict, because NO may act either as ROS scavenger or generator (favoring the synthesis of peroxynitrite), depending on the relative stoichiometry between NO and ROS [8]. This complexity may explain the discrepant reports on the effects of NO in cardiomyocytes [32],[33,34] and the different behaviour of NitDOX and FurDOX in H9c2 cells. Although we cannot infer any conclusion about the *in vivo* cardiotoxicity from these *in vitro* assays, it is noteworthy that NitDOX was a more potent cytotoxic agent than DOX and was capable to overcome drug resistance [18]. In the light of these premises, it might be administered at lower doses than DOX. Since cardiotoxicity of DOX is dose-dependent, this feature of NitDOX might decrease the risk of cumulative cardiac damages of DOX in a putative administration *in vivo*.

We cannot state that NitDOX was selective against cancer cells, since it induced the same cytotoxicity of DOX in non transformed colon epithelial cells; however, being more cytotoxic than DOX against colon cancer cells [18], NitDOX might be used *in vivo* at lower concentrations than DOX, exerting good efficacy against cancer cells and limited toxicity against colon epithelium.

An intriguing difference between DOX and NitDOX is that the latter was a less potent inhibitor of topoisomerase II, one of the known targets of anthracyclines. We postulate that the presence of nitrooxy group makes NitDOX less able to bind topoisomerase than DOX. On the other hand, this result led us to hypothesize that the cell toxicity of NitDOX was independent from topoisomerase II

inhibition and could be due to other mechanisms, such as a more favorable kinetics of uptake and/or different cellular targets.

The rate of DOX uptake was lower in drug-resistant cells than in drug-sensitive ones and was dependent on both passive diffusion and facilitated diffusion via SLC22A4, as shown by employing the SLC22A4 inhibitor TEA. High levels of SLC22A4 confer sensitivity to DOX by increasing the amount of the drug uptake by cells [21] and indeed the transporter was slightly lower in HT29-dx cells than in HT29 cells. NitDOX uptake was equal in drug-sensitive and drug-resistant cells, TEA-insensitive, appearing independent on SLC22A4, and more rapid than the uptake of DOX. NitDOX was more hydrophobic than DOX; this feature may facilitate its passive diffusion across the plasma membrane and explain its rapid uptake.

At the same time, the higher hydrophobicity limited the nuclear entry of NitDOX and favored the delivery through highly impermeant membranes, like the internal mitochondrial membrane, highlighting a second difference between DOX and NitDOX. In keeping with our observation on the mitochondrial localization of NitDOX, it has been reported that synthetic acyl-conjugated DOXs, more hydrophobic than the parental drug, are more uptaken by drug-resistant cells and display a cytosolic rather than a nuclear localization [35].

Also the level of ABC transporters in subcellular compartments, that is highly variable and cell type-dependent [36,37,38], strongly affects the intracellular distribution of anthracyclines. In our model, the rate of nitration and extrusion activity of Pgp/ABCB1, MRP1/ABCC1 and BCRP/ABCG2 did not appear to underlie the nuclear-cytosolic partition of DOX and NitDOX. Interestingly, all these ABC transporters were detected in mitochondrial extracts of HT29 and HT29-dx cells, which had a greater amount of MRP1/ABCC1. Considering the nitration pattern of MRP1/ABCC1 and BCRP/ABCG2 and the reversing effects of PTIO, which lowered the amount of mitochondrial NitDOX, we postulate that the mitochondrial retention of NitDOX also relies on the reduced efflux through ABC transporters, subsequent to their nitration.

The enhanced intramitochondrial accumulation of DOX was not peculiar of all NO-releasing molecules: the NO-donors co-incubated with DOX increased the content of DOX both in whole cell and in the nucleus, likely as a consequence of the nitration of ABC transporters in HT29 and HT29-dx cells [5,6], but did not change the DOX retention within mitochondria. Only NitE produced a slight but not significant increase of intramitochondrial DOX, which remained lower than the one obtained with NitDOX. This result suggests that the nitrooxy group conjugated with DOX is more potent as a nitrating agent of the mitochondrial ABC transporters than its ester derivative. In NitDOX, the nitrooxy group is part of a highly hydrophobic molecule; therefore it is particularly favored to cross the mitochondrial membranes delivered by such a carrier. Once entered, the mitochondrial aldehyde dehydrogenase responsible of the metabolism of nitrates can produce NO from nitrooxy group [39], increasing the intramitochondrial release of NO. As evidenced by the analysis of NitDOX metabolites in mitochondrial extracts, about 25% of NitDOX was denitrated, suggesting that NO was released from the compound within mitochondria. Of note, whereas DOX was highly converted into a more reduced metabolite suggestive of doxorubicinol [27] in both nucleus and mitochondria, the amount of NitDOX metabolized was proportionally lower. This difference, which can be due to a lower affinity of NitDOX for the catabolising enzymes, may contribute to maintain relatively high the amount of mitochondrial NitDOX.

Overall, we suggest that the different intracellular distribution of NitDOX versus DOX is the sum of at least two factors: the passive diffusion of the compound into subcellular compartments, that depends on its hydrophobicity, and the lower rate of extrusion, that relies on the activity of ABC transporters in each cell compartment. The hydrophobicity of NitDOX and the release of NO followed by the nitration of ABC transporters in mitochondria, both contribute to the high mitochondrial accumulation of NitDOX.

The mitochondrial delivery of NitDOX, which occurred in both sensitive and resistant cells, points out a novel and unexpected mechanism of cytotoxicity of this compound, in line with other works that propose a possible mitotoxic effect for some anthracyclines. For instance daunorubicin

increases the mitochondrial respiration at low concentrations and inhibits it at higher concentrations, thus acting as a mitotoxic drug [40]. Recently a liposomal daunorubicin targeting mitochondria has been shown to exert high cytotoxicity in MCF7-Adr cells in association with the calcium channel blocker amlodipine, by disrupting the mitochondrial potential, releasing the cytochrome c and activating the caspases cascade [41]. This finding confirms that the mitochondrial metabolism is critical for the survival of drug-resistant cells and is in keeping with what we observed in HT29-dx, where the TCA cycle, the electron transport across complex I and the synthesis of ATP were higher than in HT29 cells. The preferential delivery of NitDOX within mitochondria may explain its greater efficacy in inducing cytotoxicity.

It is well established that NO affects mitochondrial energy metabolism [14]. For instance it elicits the tyrosine nitration of TCA cycle enzymes like aconitase and isocitrate dehydrogenase, as well as enzymes important for the synthesis of ubiquinone and for the integrity of Fe-S clusters [42], and inhibits complex I and IV [43]. These mechanisms may account for the observed effects of NitDOX to decrease the TCA cycle, the activity of complex I and the synthesis of ATP.

Proper mitochondrial respiration protects cells against oxygen toxicity [44]. Conversely high levels of NO irreversibly damage mitochondrial respiratory chain components, resulting in oxidative and nitrosative stress, lipid peroxidation, loss of cytochrome c from permeabilized mitochondria, and activation of caspases [45]. All these events were elicited by NitDOX and relied on the release of NO from the compound, because they were prevented by PTIO. Noteworthy, a significant activation of cytochrome c/caspase-9/caspase-3 axis was achieved equally in drug-sensitive and drug-resistant cells.

In conclusion, we propose nitrooxy-doxorubicin as a new multi-target lead compound, which – originally designed as a MDR-reversing agent – has revealed a novel and unexpected mechanism of action. The simple addition of a NO-releasing group in form of nitrooxy made NitDOX a functionally distinct anthracycline, with a more favorable toxicity profile and a better efficacy against drug-resistant cells. In the context of earlier attempts to use NO-delivery strategies in cancer

therapy [46,47], we believe that NitDOX is worthy of further investigations in preclinical and clinical settings.

Acknowledgment

We are grateful to Costanzo Costamagna (Department of Oncology, University of Torino), Guido Serini (Institute for Cancer Research and Treatment, Candiolo, Italy), Erika Ortolan (Department of Genetics, Biology and Biochemistry, University of Torino) for the technical assistance.

We are grateful to dr. Silvio Aprile and Prof. Giorgio Grosa (Dipartimento di Scienze del Farmaco, Università degli Studi del Piemonte Orientale A. Avogadro, Novara, Italy) for LC-MS analysis which allowed the characterization of metabolites deriving from NitDOX.

This work has been supported with grants from the Italian Ministry of University and Research, Fondazione Internazionale Ricerche Medicina Sperimentale (FIRMS), Compagnia di San Paolo ("Progetto Oncologia"), Italian Association for Cancer Research (AIRC; MFAG 11475).

Authors also thank Prof. Alberto Gasco for fruitful discussion.

Supporting Information available

The Supporting Information include the structure of DOX, NitDOX, FurDOX, NitE and FurE (Supplementary Figure S1), the effects of the association of DOX and NO-donors (Supplementary Figure S2), the cytotoxic effects of DOX, NitDOX and FurDOX in different drug-sensitive/drug-resistant cell lines and in cardiomyocyte cultures (Supplementary Figure S3), the effects of DOX, NitDOX and FurDOX in non transformed colon epithelial cells (Supplementary Figure S4), the effects of NO-donors in the intracellular localization of DOX (Supplementary Figure S5), the representative chromatograms of the RP-HPLC analysis of DOX, NitDOX and their metabolites in cellular fractions (Supplementary Figure S6), the LC-ESI-MS analysis of DOX, NitDOX and their metabolites in cellular fractions (Supplementary Figure S7), the structures of the metabolites

generated from DOX and NitDOX (Supplementary Figure S8). This information is available free of charge via the Internet at http://pubs.acs.org.

References

1. Apetoh, L.; Mignot, G.; Panaretakis, T.; Kroemer, G.; Zitvogel, L. Immunogenicity of anthracyclines: moving towards more personalized medicine. *Trends Mol. Med.* **2008**, *14*, 141–151.
2. Gottesman, M.M.; Fojo, T.; Bates, S.E. Multidrug resistance in cancer: role of ATP-dependent transporters. *Nat. Rev. Cancer.* **2002,** *2*, 48–58.
3. Takara, K.; Sakaeda, T.; Okumura, K. An update on overcoming MDR1-mediated multidrug resistance in cancer chemotherapy. *Curr. Pharm. Des.* **2006**, *12,* 273–286.
4. Haouala, A.; Rumpold, H.; Untergasser, G.; Buclin, T.; Ris, H.B.; Widmer. N.; Decosterd, L,A. siRNA-mediated knock-down of P-glycoprotein expression reveals distinct cellular disposition of anticancer tyrosine kinases inhibitors. *Drug Metab. Lett*. **2010,** *4*, 114–119.
5. Riganti, C.; Miraglia, E.; Viarisio, D.; Costamagna, C.; Pescarmona, G.; Ghigo, D.; Bosia, A. Nitric oxide reverts the resistance to doxorubicin in human colon cancer cells by inhibiting the drug efflux. *Cancer Res.* **2005,** *65,* 516–525.
6. De Boo, S.; Kopecka, J.; Brusa, D.; Gazzano, E.; Matera, L.; Ghigo, D.; Bosia, A.; Riganti, C. iNOS activity is necessary for the cytotoxic and immunogenic effects of doxorubicin in human colon cancer cells. *Mol Cancer* **2009,** *8,* e108.
7. Fruttero, R.; Crosetti, M.; Chegaev, K.; Guglielmo, S.; Gasco, A.; Berardi, F.; Niso, M.; Perrone, R.; Panaro, M.A.; Colabufo, N.A. Phenylsulfonylfuroxans as modulators of multidrug-resistance-associated protein-1 and P-glycoprotein. *J. Med. Chem.* **2010,** *53,* 5467–575.
8. Wink, D.A.; Mitchell, J.R. Chemical biology of nitric oxide: insights into regulatory, cytotoxic and cytoprotective mechanism of nitric oxide. *Free Radic. Biol. Med.* **1998,** *25,* 434–456.

9. Nathan, C.; Xie, Q.W. Regulation of biosynthesis of nitric oxide. *J. Biol. Chem.* **1994,** *269,* 13725–13728.
10. Fitzpatrick, B.; Mehibel, M.; Cowen, R.L.; Stratford, I.J. iNOS as a therapeutic target for treatment of human tumors. *Nitric Oxide* **2008,** *19,* 217–224.
11. Singh, S.; Gupta, A.K. Nitric oxide: role in tumour biology and iNOS/NO-based anticancer therapies. *Cancer Chemother. Pharmacol*. **2011,** *67,* 1211–1224.
12. Coulter, J.A.; McCarthy, H.O.; Xiang, J.; Roedl, W.; Wagner, E.; Robson, T.; Hirst, D.G. Nitric oxide-A novel therapeutic for cancer. *Nitric Oxide* **2008,** *19,* 192–198.
13. Engels, K.; Knauer, S.K.; Loibl, S.; Fetz, V.; Harter, P.; Schweitzer, A.; Fisseler-Eckhoff, A.; Kommoss, F.; Hanker, L.; Nekljudova, V.; Hermanns, I.; Kleinert, H.; Mann, W.; du Bois, A.; Stauber, R.H. NO signaling confers cytoprotectivity through the survivin network in ovarian carcinomas. *Cancer Res.* **2008,** *68,* 5159–5166.
14. Huerta, S.; Chilka, S.; Bonavida, B. Nitric oxide donors: Novel cancer therapeutics. *Int. J. Oncol.* **2008,** *33,* 909–927.
15. Bonavida, B.; Khineche, S.; Huerta-Yepez, S.; Garbàn, H. Therapeutic potential of nitric oxide in cancer. *Drug Resist. Updat.* **2006,** *9,* 157–173.
16. Muir, C.P.; Adams, M.A.; Graham, C.H. Nitric oxide attenuates resistance to doxorubicin in three-dimensional aggregates of human breast carcinoma cells. *Breast Cancer Res. Treat.* **2006,** *96,* 169–176.
17. Frederiksen, L.J.; Sullivan, R.; Maxwell, L.R.; Macdonald-Goodfellow, S.K.; Adams, M.A.; Bennett, B.M.; Siemens, D.R.; Graham, C.H. Chemosensitization of cancer in vitro and in vivo by nitric oxide signaling. *Clin. Cancer Res.* **2007,** *13,* 2199–2206.
18. Chegaev, K.; Riganti, C.; Lazzarato, L.; Rolando, B.; Guglielmo, S.; Campia, I.; Fruttero, R.; Bosia, A.; Gasco, A. Nitric oxide donor – doxorubicin conjugates accumulate into doxorubicin resistant human colon cancer cells inducing cytotoxicity. *ACS Med. Chem. Letters* **2011,** *2,* 494–497.

19. Morphy, R.; Rankovic, Z. Designed multiple ligands. An emerging drug discovery paradigm. *J. Med. Chem.* **2005,** *48*, 6523–6543.
20. Riganti, C.; Orecchia, S.; Pescarmona, G.; Betta, P.G.; Ghigo, D.; Bosia, A. Statins revert doxorubicin resistance via nitric oxide in malignant mesotelioma. *Int. J. Cancer* **2006,** *119,* 17–27.
21. Okabe, M.; Szakàcs, G.; Reimers, M.A.; Suzuki, T.; Hall, M.D.; Abe, T.; Weinstein, J.N.; Gottesman, M.M. Profiling SLCO and SLC22 genes in the NCI-60 cancer cell lines to identify drug uptake transporters. *Mol. Cancer Ther.* **2008,** *7,* 3081–3091.
22. Campia, I.; Lussiana, C.; Pescarmona, G.; Ghigo, D.; Bosia, A.; Riganti, C. Geranylgeraniol prevents the cytotoxic effects of mevastatin in THP-1 cells, without decreasing the beneficial effects on cholesterol synthesis. *Br. J. Pharmacol.* **2009,** *158,* 1777–1786.
23. Wibom, R.; Hagenfeldt, L.; von Dobeln, U. Measurement of ATP production and respiratory chain enzyme activities in mitochondria isolated from small muscle biopsy samples. *Anal. Biochem.* **2002,** *311,* 139–151.
24. Riganti, C.; Gazzano, E.; Polimeni, M.; Costamagna, C.; Bosia, A.; Ghigo, D. Diphenyleneiodonium inhibits the cell reDOX metabolism and induces oxidative stress. *J. Biol. Chem.* **2004**, *279*, 47726–47731.
25. Ischiropoulos, H. Biological selectivity and functional aspects of protein tyrosine nitration. *Biochem. Biophys. Res., Commun.* **2003,** *305,* 776–783.
26. Russo, P.; Catassi, A.; Malacarne, D.; Margaritora, S.; Cesario, A.; Festi, L.; Mulé, A.; Ferri, L.; Granone, P. Tumor necrosis factor enhances sn38-mediated apoptosis in mesothelioma cells. *Cancer* **2005,** *103,* 1503–1518.
27. Sakai Kato, K.; Saito, E.; Ishikura, K.; Kawanishi, T. Analysis of intracellular doxorubicin and its metabolites by ultrahighperformance liquid chromatography. *J. Chromatogr. B Analyt. Technol. Biomed. Life Sci.* **2010,** *878,* 1466–1470.

28. Rothweiler, F.; Michaelis, M.; Brauer, P.; Otte, J.; Weber, K.; Fehse, B.; Doerr, H.W.; Wiese, M.; Kreuter, J.; Al-Abed, Y.; Nicoletti, F.; Cinatl. J. Anticancer effects of the nitric oxide-modified saquinavir derivative saquinavir-NO against multidrug-resistant cancer cells. *Carcinogenesis* **2012,** *12,* 1023-1030.
29. Colabufo, N.A.; Contino, M.; Berardi, F.; Perrone, R.; Panaro, M.A.; Cianciulli, A.; Mitolo, V.; Azzariti, A.; Quatrale, A.; Paradiso, A. A new generation of MDR modulating agents with dual activity: P-gp inhibitor and iNOS inducer agents. *Toxicol. in Vitro* **2011,** *25,* 222–230.
30. Rao, C,V. Nitric oxide signaling in colon cancer chemoprevention. *Mutation Res.* **2004,** *555,* 107–119.
31. Hagos, G.K., Carroll, R.E., Kouznetsova, T., Li, Q., Toader, V., Fernandez, P.A., Swanson, S.M., Thatcher, G.R.J. Colon cancer chemoprevention by a novel NO chimera that shows anti-inflammatory and antiproliferative activity in vitro and in vivo. *Mol. Cancer Ther.* **2007,** *6,* 2230–2239.
32. Aldieri, E.; Bergandi, L.; Riganti, C.; Costamagna, C.; Bosia, A.; Ghigo, D. Doxorubicin induces an increase of nitric oxide synthesis in rat cardiac cells that is inhibited by iron supplementation. *Toxicol. Appl. Pharmacol.* **2002,** *185,* 85–90.
33. Evig, C.B.; Kelley, E.E.; Weydert, C.J.; Chu, Y.; Buettner, G.R.; Burns, C.P. Endogenous production and exogenous exposure to nitric oxide augment doxorubicin cytotoxicity for breast cancer cells but not cardiac myoblasts. *Nitric Oxide* **2004,** *10,* 119–129.
34. Zhu, S.G.; Kukreja, R.C.; Das, A.; Chen, Q.; Lesnefsky, E.J.; Xi, L. Dietary nitrate supplementation protects against doxorubicin-induced cardiomyopathy by improving mitochondrial function. *J. Am. Coll. Cardiol.* **2011,** *57,* 2181–2189.
35. Effenberger-Neidnicht, K.; Breyer, S.; Mahal, K.; Sasse, F.; Schobert, R. Modification of uptake and subcellular distribution of doxorubicin by N-acylhydrazone residues as visualised by intrinsic fluorescence. *Cancer Chemother. Pharmacol.* **2012,** *69,* 85–90.

36. Solazzo, M.; Fantappiè, O.; Lasagna, N.; Sassoli, C.; Nosi, D.; Mazzanti, R. P-gp localization in mitochondria and its functional characterization in multiple drug-resistant cell lines. *Exp. Cell Res.* **2006;** *12*, 4070–4078.

37. Paterson, J.K.; Gottesman, M.M. P-glycoprotein is not present in mitochondrial membranes. *Exp Cell Res.* **2007,** *313*, 3100–3105.

38. Solazzo, M.; Fantappiè, O.; D'Amico, M.; Sassoli, C.; Tani, A.; Cipriani, G.; Bogani, C.; Formigli, L.; Mazzanti, R. Mitochondrial expression and functional activity of breast cancer resistance protein in different multiple drug-resistant cell lines. *Cancer Res.* **2009,** *69*, 7235–7242.

39. Mayer, B.; Beretta, M. The enigma of nitroglycerin bioactivation and nitrate tolerance: news, views and troubles. *Br. J. Pharmacol.* **2008,** *155*, 170–184.

40. Paul, M.K.; Patkari, M.; Mukhopadhayay, A.P. Existence of a distinct concentration window governing daunorubicin-induced mammalian liver mitotoxicity-implication for determining therapeutic window. *Biochem. Pharmacol.* **2007,** *74*, 821–830.

41. Zhang, Y.; Li, R.J.; Ying, X.; Tian, W.; Yao, H.J.; Men, Y.; Yu, Y.; Zhang, L.; Ju, R.J.; Wang, X.X.; Zhou, J.; Chen, J.X.; Li, N.; Lu, W.L. Targeting therapy with mitosomal daunorubicin plus amlodipine has the potential to circumvent intrinsic resistant breast cancer. *Mol. Pharm.* **2011,** *8*, 162–175.

42. Bhattacharjee, A.; Majumdar, U.; Maity, D.; Subhra Sarkar, T.; Mohan Goswami, A.; Sahoo, R.; Ghosh, S. In vivo protein tyrosine nitration in S. cerevisiae: Identification of tyrosine-nitrated proteins in mitochondria. *Biochem. Biophys. Res. Commun.* **2009,** *388*, 612–617.

43. Sarti, P.; Arese, M.; Forte, E.; Giuffrè, A.; Mastronicola, D. Mitochondria and nitric oxide: chemistry and pathophysiology. *Adv. Exp. Med. Biol.* **2012,** *942*, 75–92.

44. Sung, H.J.; Ma, W.; Wang, P.; Hynes, J.; O'Riordan, T.C.; Combs, C.A.; McCoy, J.P.; Bunz, F.; Kang, J.G.; Hwang, P.M. Mitochondrial respiration protects against oxygen-associated DNA damage. *Nat. Commun.* **2010,** *1*, 5, doi: 10.1038/ncomms1003.

45. Kim, P.K.M.; Kwon, Y.G.; Chung, H.T.; Kim, Y.M. Regulation of caspases by nitric oxide. *Ann. N.Y. Acad. Sci.* **2002,** *962,* 42–52.

46. Sonveaux, P.; Jordan, B.F.; Gallez, B.; Feron, O. Nitric oxide delivery to cancer: Why and how? *Eur. J. Cancer.* **2009,** *45,* 1352–1369

47. Siemens, D.R.; Heaton, J.P.; Adams, M.A.; Kawakami, J.; Graham, C.H. Phase II study of nitric oxide donor for men with increasing prostate-specific antigen level after surgery or radiotherapy for prostate cancer. *Urology* **2009,** *74,* 878–883.

Table 1

Quantitation by HPLC analysis of DOX, NitDOX, and metabolites in the cellular fractions (cytosolic, mitochondrial and nuclear extracts) from HT29 cells incubated with 10 µmol/L doxorubicin (DOX) or nitrooxy-doxorubicin (NitDOX) for 24 h. Values are the average of five experiments (n = 5, SD < 0.6) for NitDOX.

Cellular fractions	Incubated compounds	detected compounds after 24 hours incubation (nmol/mg prot.)		
		NitDOX	DOX	other metabolites
Cytosol	**DOX**	-	ND [a]	ND [a]
	NitDOX	3.5	ND [a]	1.1 **(NitDOX denitrate 1 and 2)**
Mitochondria	**DOX**	-	6.2	4.5 **(DOX-ol)**
	NitDOX	15.5	3.6	6.0 **(NitDOX denitrate and 2)**
Nucleus	**DOX**	-	8.8	5.3 **(DOX-ol)**
	NitDOX	1.2	ND [a]	0.6 **(NitDOX denitrate 1 and 2)**

[a] *ND= not detectable (absent or < 0.5 nmol/mg prot.)*

Figure legends

Figure 1. Effects of doxorubicin and NO-releasing doxorubicins in sensitive and resistant cells.

A. Expression of ABC transporters in DOX-sensitive human colon cancer HT29 cells and DOX-resistant HT29-dx cells. Cells were lysed and the whole cellular lysate was subjected to Western blotting for Pgp/ABCB1, MRP1/ABCC1, MRP2/ABCC2 and BCRP/ABCG2 proteins (see Experimental Section). The expression of actin, as product of an housekeeping gene, was used as a control of equal protein loading. The figure is representative of three experiments with similar results. **B.C.D.** HT29 and HT29-dx cells were cultured in fresh medium (*0*) or in the presence of 5 μmol/L DOX (*DOX*), nitrooxy-DOX (*NitDOX*) or 3-phenylsulfonylfuroxan-DOX (*FurDOX*) for 1, 3, 6, 24 h. The intracellular accumulation of DOXs (panel **B**) was measured fluorimetrically in cell lysates, the amount of extracellular nitrite (panel **C**) and the release of LDH (panel **D**) were evaluated as reported in the Experimental Section. In panel **C**: the scale on the left y-axis refers to DOX and NitDOX, the scale on the right y-axis refers to FurDOX. Measurements were performed in triplicate and data are presented as means $\pm$ SD (n = 3). Versus untreated cells (*0*): * $p < 0.05$. Versus DOX alone in the same dataset: ° $p < 0.05$.

Figure 2. *In vitro* topoisomerase II inhibition by doxorubicin and nitrooxy-doxorubicin.

The activity of human purified topoisomerase II was measured after incubating the enzyme with the supercoiled pHOT1 plasmid, in the absence (*C*) or presence of DOX (1, 5, 25, 50 μmol/L, *DOX*) or nitrooxy-DOX (1, 5, 25, 50 μmol/L, *NitDOX*). Etoposide (5, 50, 100 μmol/L, *etop*) was used as positive control of topoisomerase inhibition. The reaction products were resolved on agarose gel. Linear pHOT1 (lane *P*) was used as a marker. To obtain a blank, supercoiled pHOT1 was incubated in the absence of topoisomerase II (lane C^-). *N*: nicked pHOT1; *L*: linear pHOT1; *S*: supercoiled pHOT1.

Figure 3. Doxorubicin and nitrooxy-doxorubicin uptake and intracellular distribution.

A. DOX-sensitive HT29 cells and DOX-resistant HT29-dx cells were incubated for 10 min with 5 μmol/L DOX (*DOX*) or nitrooxy-DOX (*NitDOX*), in the absence or presence of 100 μmol/L tetraethylammonium chloride (*TEA*), then washed and analysed fluorimetrically for the intracellular drug content. Measurements were performed in triplicate and data are presented as means ± SD (n = 3). HT29-dx *DOX* versus HT29 *DOX*: * $p < 0.002$; *DOX* versus *DOX*+*TEA*: ° $p < 0.05$; *NitDOX* versus the respective condition with *DOX*; $^{\lozenge}$ $p < 0.002$. **B**. Expression of SLC22A4 in HT29 and HT29-dx cells. Whole cellular lysate was analysed by Western blotting for SLC22A4 protein, using the expression of actin as a control of equal protein loading. The figure is representative of three experiments with similar results. **C**. Confocal microscope analysis of intracellular DOX. Non-permeabilized HT29 cells were incubated 24 h with 5 μmol/L DOX (*DOX*) or nitrooxy-DOX (*NitDOX*) and counterstained with DAPI. Image acquisition was performed with a Leica TCS SP2 AOBS confocal laser-scanning microscope (Leica Microsystems, Wetzlar, Germany) with a 63 x oil immersion objective and 10 x ocular lens.The micrographs are representative of three experiments with similar results. **D.** Nuclear and cytosolic content of DOXs. HT29 and HT29-dx cells were treated for 24 h with 5 μmol/L DOX (*DOX*) or nitrooxy-DOX (*NitDOX*); nuclear and cytosolic extracts were prepared as reported under Experimental Section and checked for the intracellular drug content by fluorimetric assay. Measurements were performed in triplicate and data are presented as means ± SD (n = 3). *NitDOX* versus *DOX* in nucleus: * $p < 0.001$; *NitDOX* versus *DOX* in cytosol: ° $p < 0.001$.

Figure 4. Mitochondrial accumulation of doxorubicin and nitrooxy-doxorubicin.

A. Subcellular localization of nitrooxy-DOX. HT29 cells were incubated 18 h with the expression vectors encoding for the GFP-fused-leader sequence of E1 α pyruvate dehydrogenase (to label mitochondria), the GFP-fused-KDEL sequence of calreticulin (to label endoplasmic reticulum), the GFP-fused N-acetylgalactosaminyltransferase 2 (to label Golgi apparatus), then incubated for 6 h

with 10 µM nitrooxy-DOX (*NitDOX*) and analysed by Olympus FV300 laser scanning confocal microscope (Olympus Biosystems, Hamburg, Germany). Cells were imaged using a 60 x oil immersion objective and 10 x ocular lens. Nomarski images were obtained by differential interference contrast optical components installed on an IX71 inverted microscope. The micrographs are representative of three experiments with similar results. **B.** HT29 and HT29-dx cells were incubated with 5 µmol/L DOX (*DOX*) or nitrooxy-DOX (*NitDOX*), in the absence or presence of the NO scavenger PTIO (100 µmol/L), then fractioned. The mitochondria extracts were analyzed fluorimetrically to measure the DOXs amount. Measurements were performed in triplicate and data are presented as means $\pm$ SD (n = 3). *NitDOX* versus *DOX*: * $p < 0.001$; *NitDOX+PTIO* versus *NitDOX alone*: ° $p < 0.002$. **C.** Western blot detection of nitrated mitochondrial ABC transporters. Mitochondrial extracts from cells untreated (*ctrl*) or treated as reported in panel **B** were lysed and immunoprecipitated with an anti-nitrotyrosine polyclonal antibody. The immunoprecipitated proteins were subjected to Western blotting, using anti-Pgp/ABCB1, anti-MRP1/ABCC1, anti-MRP2/ABCC2 or BCRP/ABCG2 antibodies (see Experimental Section). An aliquot of each sample was tested with the same antibodies before immunoprecipitation, to measure the amount of total ABC transporters. Porin was used as control of equal protein loading. The figure is representative of three similar experiments.

Figure 5. Effects of doxorubicin and nitrooxy-doxorubicin on mitochondrial metabolism.
HT29 and HT29-dx cells were grown for 24 h in fresh medium (*ctrl*) or with 5 µmol/L DOX (*DOX*) or nitrooxy-DOX (*NitDOX*), in the absence or presence of the NO scavenger PTIO (100 µmol/L), then subjceted to the following investigations.
A. Tricarboxylic acid cycle was measured in living cells, labelled with [14-^{6}C]-glucose, as reported in the Experimental Section. Measurements were performed in triplicate and data are presented as means $\pm$ SD (n = 3). Versus *ctrl* HT29: * $p < 0.005$; versus *ctrl* HT29-dx : ° $p < 0.001$; *DOX +PTIO* or *NitDOX+PTIO* versus *DOX* or *NitDOX* alone: $^{\lozenge}$ $p < 0.01$. **C-E.** Isolated mitochondria were

analysed for the activity of complex I (panel **B**), complex I+II (panel **C**), complex II+III (panel **D**), complex IV (panel **E**). Measurements were performed in triplicate and data are presented as means ± SD (n = 3). Versus *ctrl* HT29: * $p < 0.01$; versus *ctrl* HT29-dx: ° $p < 0.005$; *DOX +PTIO* or *NitDOX+PTIO* versus *DOX* or *NitDOX* alone: $^{\diamond}$ $p < 0.05$. **F.** ATP levels were detected by a chemiluminescence-based assay as described under Experimental Section. Measurements were performed in triplicate and data are presented as means ± SD (n = 3). Versus *ctrl* HT29: * $p < 0.02$; versus *ctrl* HT29-dx: ° $p < 0.001$; *DOX +PTIO* or *NitDOX+PTIO* versus *DOX* or *NitDOX* alone: $^{\diamond}$ $p < 0.02$.

Figure 6. Effects of doxorubicin and nitrooxy-doxorubicin on the synthesis of ROS and RNS. HT29 and HT29-dx cells were grown for 24 h in fresh medium (*ctrl*) or with 5 μmol/L DOX (*DOX*) or nitrooxy-DOX (*NitDOX*). When indicated the NO scavenger PTIO (100 μmol/L) was added. **A.** ROS levels. Cells were incubated for 20 min at 37°C with the ROS-sensitive probe DCFDA-AM, then analysed by flow cytometry in duplicate (n = 3). The histograms depict one representative experiment (*grey curve*: untreated cells; *dotted line*: DOX-treated cells; *continuous line*: NitDOX-treated cells). **B.** RNS levels. The intracellular amount of nitrotyrosine, taken as an index of RNS, was detected in cell lysates by an ELISA kit (see Experimental Section). Measurements were performed in triplicate and data are presented as means ± SD (n = 3). Versus *ctrl* HT29: * $p < 0.001$; versus *ctrl* HT29-dx : ° $p < 0.02$. **C.** Lipoperoxidation measurement. The amount of MDA, a marker of lipid peroxidation, was measured in the cell lysates spectrophometrically, as described in the Experimental Section. Measurements were performed in triplicate and data are presented as means ± SD (n = 3). Versus *ctrl* HT29: * $p < 0.001$; *NitDOX+PTIO* versus *NitDOX* alone: ° $p < 0.05$.

Figure 7. Induction of apoptosis by nitrooxy-doxorubicin in sensitive and resistant cells.

HT29 and HT29-dx cells were grown for 24 h in fresh medium (*ctrl*) or with 5 μmol/L DOX (*DOX*) or nitrooxy-DOX (*NitDOX*), in the absence or presence of the NO scavenger PTIO (100 μmol/L, *PT*), then subjected to the following investigations.

A.Citochrome c release. Cytosol and mitochondrial fractions were separated and subjected to Western blotting analysis for cytochrome c. Porin and actin were used as equal loading controls for each fraction. The figure is representative of three experiments with similar results. **B-C.** The activity of caspase-9 (panel **B**) and caspase-3 (panel **C**) was measured fluorimetrically in cell lysates, as reported under Experimental Section. Measurements were performed in triplicate and data are presented as means $\pm$ SD (n = 3). Versus *ctrl*: * $p < 0.05$; *DOX +PTIO* or *NitDOX +PTIO* versus *DOX* or *NitDOX* alone: ° $p < 0.05$.